



# Sonochemical degradation of ethyl paraben in environmental samples: Statistically important parameters determining kinetics, by-products and pathways



Costas Papadopoulos<sup>a</sup>, Zacharias Frontistis<sup>a</sup>, Maria Antonopoulou<sup>b</sup>, Danae Venieri<sup>c</sup>, Ioannis Konstantinou<sup>b</sup>, Dionissios Mantzavinos<sup>a,\*</sup>

<sup>a</sup> Department of Chemical Engineering, University of Patras, Caratheodory 1, University Campus, GR-26504 Patras, Greece

<sup>b</sup> Department of Environmental & Natural Resources Management, University of Patras, 2 Seferi St., GR-30100 Agrinio, Greece

<sup>c</sup> School of Environmental Engineering, Technical University of Crete, Polytechniopolis, GR-73100 Chania, Greece

## ARTICLE INFO

### Article history:

Received 28 August 2015

Received in revised form 3 November 2015

Accepted 4 December 2015

Available online 8 December 2015

### Keywords:

Sonodegradation  
Factorial design  
Intermediates  
Micro-pollutants  
Aqueous matrix  
Estrogenicity

## ABSTRACT

The sonochemical degradation of ethyl paraben (EP), a representative of the parabens family, was investigated. Experiments were conducted at constant ultrasound frequency of 20 kHz and liquid bulk temperature of 30 °C in the following range of experimental conditions: EP concentration 250–1250 µg/L, ultrasound (US) density 20–60 W/L, reaction time up to 120 min, initial pH 3–8 and sodium persulfate 0–100 mg/L, either in ultrapure water or secondary treated wastewater.

A factorial design methodology was adopted to elucidate the statistically important effects and their interactions and a full empirical model comprising seventeen terms was originally developed. Omitting several terms of lower significance, a reduced model that can reliably simulate the process was finally proposed; this includes EP concentration, reaction time, power density and initial pH, as well as the interactions (EP concentration) × (US density), (EP concentration) × (pH<sub>0</sub>) and (EP concentration) × (time).

Experiments at an increased EP concentration of 3.5 mg/L were also performed to identify degradation by-products. LC-TOF-MS analysis revealed that EP sonochemical degradation occurs through dealkylation of the ethyl chain to form methyl paraben, while successive hydroxylation of the aromatic ring yields 4-hydroxybenzoic, 2,4-dihydroxybenzoic and 3,4-dihydroxybenzoic acids. By-products are less toxic to bacterium *V. fischeri* than the parent compound.

© 2015 Elsevier B.V. All rights reserved.

## 1. Introduction

Parabens, esters of 4-hydroxybenzoic acid with an alkyl (from ethyl to butyl) or benzyl group, have been employed for about a century as preservatives in foodstuff, cosmetics and pharmaceuticals and personal care products [1]. Several studies published at the turn of the millennium suggested possible estrogenic activity [2,3] and carcinogenic potential [4]. In this respect and although parabens were generally considered harmless to human beings for a long time, several concerns have been raised over the past twenty years about parabens safety with emphasis given on their endocrine disrupting potential [5].

Monitoring campaigns in wastewater treatment plants (WWTPs) in Europe, North America and Japan showed influent

concentrations at the ng/L level, although in certain cases these reached the µg/L level [5]. Parabens are not adsorbed in the sludge and mostly remain in the liquid phase where they can be degraded relatively easily but not completely [6]; therefore, WWTPs are considered the major point source of parabens in the environment due to their incomplete removal [5]. Consequently, parabens re-enter the aquatic environment and they are typically found at the ng/L level [1].

Unlike other emerging micro-pollutants, the advanced oxidation of parabens has received considerably less attention possibly due to the facts that (i) suitable detection techniques were only developed in the past 10–15 years [1], and (ii) their adverse effects to living organisms are still arguable. Steter et al. [7] studied the electrochemical oxidation of methyl paraben on boron-doped diamond, while Hernandez-Leal et al. [8] studied the removal of four parabens with C1–C4 alkyl groups by ozonation or activated carbon adsorption in various water matrices. Dobrin et al. [9]

\* Corresponding author.

E-mail address: [mantzavinos@chemeng.upatras.gr](mailto:mantzavinos@chemeng.upatras.gr) (D. Mantzavinos).

proposed a hybrid system coupling non-thermal plasma and ozonation to degrade methyl paraben and concluded that the integrated process was more effective than the individual ones in terms of mineralization. Furthermore, several photochemical [10] and TiO<sub>2</sub>-based photocatalytic processes [11–13] have also been tested to degrade various parabens.

In recent years, ultrasound irradiation has been widely employed to degrade successfully various micro-pollutants including endocrine disrupting compounds (EDCs) such as bisphenol A [14,15], estrogens [16,17], 4-cumylphenol [18] and phthalates [19]. Nevertheless, the literature on the sonochemical degradation of parabens is very limited consisting only of a couple of recent studies. Sasi et al. [20] investigated the high frequency (200–1000 kHz) sonochemical degradation of methyl paraben with emphasis on the effect of operating variables and the water matrix, while Daghri et al. [21] reported that the sonochemical degradation of butyl paraben at 518 kHz was enhanced when the system was simultaneously irradiated by UV-C light.

The purpose of this work was to study the low frequency (20 kHz) sonochemical degradation of ethyl paraben (EP) and evaluate the statistically significant parameters that may determine degradation rates implementing a factorial design methodology. Six parameters were tested, namely EP concentration, ultrasound power, reaction time, water matrix, initial pH and the addition of sodium persulfate. Early-stage transformation by-products were also identified and a plausible reaction network was suggested.

## 2. Materials and methods

### 2.1. Materials

Ethyl paraben (EP) (HO–C<sub>6</sub>H<sub>4</sub>–CO–O–CH<sub>2</sub>CH<sub>3</sub>, CAS no: 120-47-8) and sodium persulfate (SPS) (Na<sub>2</sub>S<sub>2</sub>O<sub>8</sub>, 99+%, CAS number 7775-27-1) were supplied by Sigma–Aldrich and used as received. Two water matrices were employed, i.e. ultrapure water (UPW, pH = 6.5) taken from a water purification system (EASYPureRF-Barnstead/ThermoFisher, USA), and secondary treated wastewater (WW) taken from the university campus treatment plant (pH = 8, COD = 21 mg/L). Sulfuric acid or sodium hydroxide was used, as needed, to adjust the initial solution pH of about 6 to acidic or alkaline conditions.

### 2.2. Ultrasound irradiation

A Branson 450 horn-type digital sonifier operating at a fixed frequency of 20 kHz was employed. Reactions took place in a cylindrical, double-walled, Pyrex vessel, which was open to the atmosphere. Ultrasound irradiation was emitted through a 1 cm in diameter titanium tip which was positioned in the middle of the vessel at a distance of 3 cm from the bottom. The working volume was 0.12 L and the bulk temperature was kept constant at 30 °C with a temperature control unit. The maximum nominal power output of the sonifier was 450 W and the actual energy transmitted to the liquid phase was determined calorimetrically; experiments were performed at actual power densities of 20 and 60 W/L.

### 2.3. Chromatographic techniques

High performance liquid chromatography (HPLC: Alliance 2695, Waters) was employed to monitor the concentration of EP. Separation was achieved on a Kinetex XB-C18 100A column (2.6 μm, 2.1 mm × 50 mm) and a 0.5 μm inline filter (KrudKatcher Ultra) both purchased from Phenomenex. The mobile phase consisting of 75:25 water:acetonitrile eluted isocratically at 0.35 mL/min and 45 °C, while the injection volume was 40 μL. Detection was

achieved through a photodiode array detector (Waters 2996 PDA detector, detection λ = 254 nm).

The evolution of sulfate ions during the process was followed by a Dionex ICS-1500 instrument equipped with an ASRS Ultra II conductivity detector and IonPac AS9-HC anionic column. The mobile phase was an aqueous sodium carbonate (9 mM) solution at a flow rate of 1 mL/min, while the injection volume was 25 μL.

LC–TOF–MS (liquid chromatography–time of flight mass spectrometry) system was applied for the identification of transformation by-products (TBPs) of EP. Prior to analysis, 2 mL of treated solutions were extracted by means of a solid-phase extraction (SPE), reported in our previous work [12], using Oasis HLB (divinyl benzene/N-vinylpyrrolidone copolymer) cartridges (60 mg, 3 mL) from Waters (Mildford, MA, USA). The LC system consisted of an Ultra-High Performance LC pump (Dionex Ultimate 3000, Thermo) incorporating a column thermostat and an autosampler interfaced to a Focus microTOF II – time of flight mass spectrometer (Bruker Daltonics, Germany). The MS part was operated using microTOF control (version 2.0) software. The scan range applied in the full-scan mode was *m/z* 50–500 at a scan rate 1 Hz. The chromatographic separations were run on a C18 Acclaim™ RSLC, 100 mm × 2.1 mm, 2.2 μm particle size (Thermo Fisher Scientific, San Jose, USA) at 30 °C. The injected sample volume was 10 μL. Mobile phases A and B were water with 0.1% formic acid and acetonitrile, respectively at a flow-rate of 0.2 mL/min. Analysis was performed by ESI source in negative ionization mode. A linear gradient progressed from 5% B (initial conditions) to 99.9% A in 12 min (maintained for 2 min), returned to the initial conditions after 1 min and finally re-equilibration time was set at 3 min. The ESI-source parameters were as follows: dry gas flow rate 8 L/min (nitrogen), nebulizer pressure 2.0 bar, capillary voltage at 3200 V, end plate offset at 500 V, collision cell RF 70.0 Vpp, dry temperature at 220 °C. Prior to analysis, the TOF mass analyzer was externally calibrated using sodium formate, in the scan range *m/z* 50–1000, to ensure mass accuracy with ±5 ppm. Data were acquired with the HyStar 3.2 software and analysed with Data Analysis 4.1 software package. In addition, chemical formula calculator, included in Data Analysis software was used to provide chemical formula and mass accuracy values. The identification of the majority of the TBPs was also verified by comparison of retention time, high resolution mass and MS spectra to the commercially available standards.

### 2.4. Acute ecotoxicity

The marine bacterium *Vibrio fischeri* was used to assess the acute ecotoxicity of EP prior to and after sonodegradation. Changes in bioluminescence of *V. fischeri* exposed to EP solutions for 15 min were measured using a LUMISTox analyzer (Dr. Lange, Germany) and the results were compared to an aqueous control.

### 2.5. Yeast estrogen screening (YES)

The YES assay using the yeast *Saccharomyces cerevisiae* was carried out to assess the estrogenicity of EP according to the procedures described in detail elsewhere [22]. In brief, standard solutions and sample extracts were produced in ethanol and 10 μL of dilution series were dispensed into triplicate wells of 96-well microtiter plates. After evaporation to dryness at room temperature, 0.2 mL of growth medium containing the chromogenic substrate chlorophenol red-β-D-galactopyranoside (CPRG) and the yeast cells were added, followed by incubation at 32 °C for 72 h. Each plate contained at least one row of blanks and a standard curve for 17β-estradiol (E2). During the incubation period, the microtiter plates were shaken at 80 rpm for 2 min to mix and disperse the growing cells. The absorbance of the medium

was measured using a microplate reader (LT-4000MS Microplate Reader, Labtech) and Manta PC analysis software. The absorbance at 540 nm was regarded as estrogenic activity after subtraction of absorbance at 620 nm to correct for yeast growth. Positive wells are indicated by a deep red color and by turbid yeast growth.

### 3. Results and discussion

#### 3.1. How estrogenic is ethyl paraben?

Although parabens have been suspected for endocrine disrupting behavior, information regarding their estrogenicity is scarce [2]. In view of this, the YES assay was employed to evaluate EP estrogenicity relative to 17 $\beta$ -estradiol (E2) and the results are shown in Fig. 1. EP is slightly estrogenic in the range of concentrations tested (i.e. 250  $\mu$ g/L–8 mg/L including the concentrations of the factorial design as will be discussed in Section 3.2); in fact, its estrogenic activity at the maximum concentration of 8 mg/L is about 4 times lower than that of reference E2 at its lowest concentration of 62.5  $\mu$ g/L. The inset of Fig. 1 shows a pictorial representation of the assay, where changes from yellow to brown to red color are characteristic of a transition from zero to moderate to intense estrogenicity. Routledge et al. [2] reported that parabens, including EP, were several times less responsive to the YES test than E2.

#### 3.2. Selection of parameters and factorial design

The rate at which organic pollutants can be degraded by sonochemical (or other advanced oxidation) processes may be affected by various parameters related to the generation of hydroxyl radicals and other reactive oxygen species (ROS), the properties and concentration of the pollutants and the water matrix itself.

For instance, both the ultrasound frequency and power density will determine the number and size of collapsing cavitation bubbles, and eventually, the concentration of ROS in the liquid bulk [23]. Of these, hydroxyl radicals are the dominant species formed through water sonolysis:



Moreover, the addition of SPS may promote degradation since recent studies have shown that ultrasound can activate SPS to produce reactive sulfate radicals [15,24,25]:

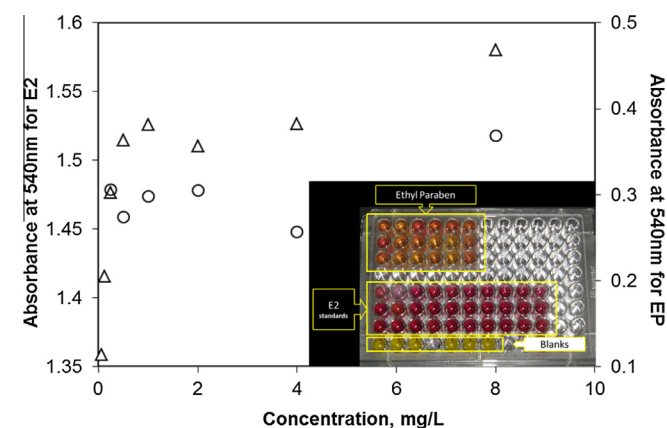
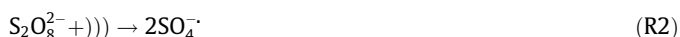


Fig. 1. Response of the YES assay to EP (–O–) and E2 (– $\Delta$ –) at various concentrations. Inset: Triplicate wells of blanks, EP and E2.

Equally important is EP concentration since the concentration ratio of continuously sono-generated ROS to batch-fed EP will determine degradation kinetics and apparent orders of reaction (as will be discussed in Section 3.3). Since emerging micro-pollutants are likely to appear in various water matrices including groundwater and WWTP effluents, the effect of matrix complexity (e.g. organic and inorganic constituents of WW) on degradation should be assessed in comparison to e.g. UPW.

Fig. 2 shows typical results concerning EP sonochemical degradation as a function of six parameters, namely: reaction time, ultrasound power density, EP concentration, water matrix and pH, and the presence of SPS. Although one could guess correctly that the amount of EP degraded depends on its initial concentration and the reaction time, the effect of other parameters may not be evident.

In this work, a statistical approach was chosen based on a factorial experimental design that would allow us to infer about the individual and combined effects of the parameters with a relatively small number of experiments. The independent parameters of the experimental design are presented in Table 1. Each one of the six variables received two values, a high value (indicated by the plus sign) and a low value (indicated by the minus sign).

EP concentration levels between the very low mg/L and low  $\mu$ g/L were chosen in this work, which (i) allows the accurate quantitation of residual EP down to few  $\mu$ g/L with the analytical techniques available in this work, and (ii) covers, to a certain degree, the environmentally relevant concentrations of parabens that take values between ng/L and  $\mu$ g/L [1,5].

The lower power density was chosen to secure a sufficient degradation rate since preliminary experiments showed little sonochemical activity below 20 W/L, while the upper power density of 60 W/L was selected to allow for the fast removal of dissipated heat, thus keeping the liquid bulk temperature constant.

The addition of SPS at 100 mg/L was based on the findings of a recent study of our group [15] regarding the sonochemical degradation of endocrine disruptor bisphenol A at similar operating conditions.

The initial pH was varied between 3 and 8, whereas the lower pH values stand for wastewaters from the cosmetics/pharmaceuticals industry, while the upper value matches that of the municipal WW sample. Although the solution was not buffered to the aforementioned pH values, pH was monitored constantly throughout the reaction showing that only marginal changes had occurred between the initial and after 120 min solutions.

Finally, the reaction timescale was selected to achieve considerable EP degradation within a reasonable period of time, according to screening experiments (i.e. Fig. 2).

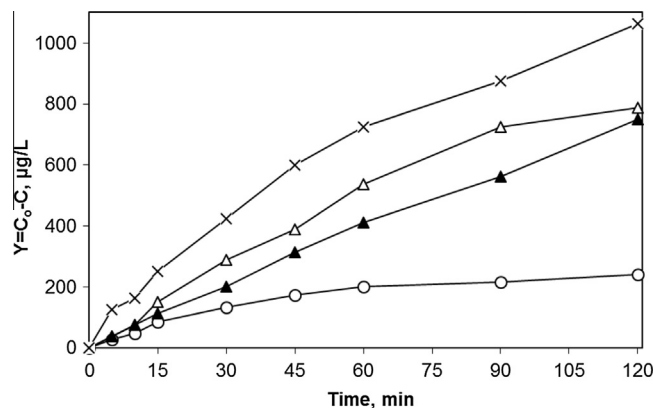


Fig. 2. Sonochemical degradation profiles of EP at various operating conditions as shown in Table 2. –O– Run 7; –X– Run 30; – $\Delta$ – Run 20; – $\blacktriangle$ – Run 10.

**Table 1**  
Independent parameters of the 2<sup>6</sup> experimental design.

Value level	EP (μg/L)	Ultrasound (US) density (W/L)	SPS (mg/L)	pH <sub>0</sub>	Water matrix	Time (min)
–1	250	20	0	3	UPW	30
+1	1250	60	100	8	WW	120

It should be noted that the ultrasound frequency was not selected as a process variable but kept fixed at 20 kHz due to lack of equipment operating at higher frequencies. In recent studies, various EDCs have been treated by both high (i.e. in the range 300–1200 kHz [14,18–20]) and low (i.e. 20–80 kHz [15–17]) frequency ultrasound. High frequencies (at about 300 kHz) can produce more free radicals in the liquid bulk [23], thus oxidizing faster hydrophilic and non-volatile compounds such as EP (whose solubility is 885 mg/L and the vapor pressure is 0.01239 Pa at 25 °C [1]). On the contrary, low frequencies yield more violent cavitation with increased localized temperatures and pressures, thus promoting thermal reactions inside and/or close to the bubble. Overall, the effect of frequency is case-specific and interdependent to the physicochemical properties of the substrate, the level of operating power density and the relative concentration of ROS to substrate (the latter will be discussed in Section 3.3).

Table 2 shows the 2<sup>6</sup> experimental design followed in this work, alongside the response (dependent variable), *Y*, in terms of μg/L of EP removed. It should be noted here that for experimental designs where the pollutant concentration is one of the independent parameters, it is not advisable to use the per cent conversion as the response factor. Conversion, depending on the degradation kinetics (see Section 3.3), will either remain constant or decrease with increasing concentration although the mass of pollutant destroyed may, at the same time, increase. From an environmental perspective, the key factor should be the amount of pollutant removed rather than its conversion.

Estimation of the average effect, the main effects and the two and higher order interactions of the operating factors studied was made by means of the statistical package Minitab 17. The results are presented in Table 3. To assess the significance of the effects, an estimate of the standard error is required. An estimate of the standard error is usually made by performing repeat runs. Alternatively, three and higher order interactions can be used, since these interactions may be considered negligible and may measure differences arising from experimental error [26]. The variance of each effect would then be:

$$\text{Variance of effects} = \frac{\sum (\text{three and higher order effect})^2}{\text{Number of three and higher order effects}} \quad (\text{E1})$$

The standard error is then the square root of the variance (half this amount for the average). If an effect is about or below the standard error, it may be considered insignificant. The contribution of a parameter, however, whose effect appears different from zero, is not necessarily very large. One way to identify the most important effects is to construct the normal probability plot [26,27], where small effects will appear on a straight line. Any effects with a significant contribution will lie away from the normal probability line. The normal probability plot for the degradation of EP appears in Fig. 3a. With the exception of water matrix, the other five parameters appear to have an effect on EP degradation; the effects are positive indicating that an increase in their level brings about an increase in the amount of EP removed. Second order interactions between (EP concentration) × (US density), (EP concentration) × (pH<sub>0</sub>) and (EP concentration) × (time) also appear to

**Table 2**  
Observed response *Y* (μg/L of EP removed) and pseudo-first order kinetic constant (min<sup>–1</sup>) for the 2<sup>6</sup> factorial experimental design. Numbers in brackets show linear regression coefficient *R*<sup>2</sup> (%).

Run no	EP	Ultrasound (US) density	SPS	pH <sub>0</sub>	Water matrix	Time	<i>Y</i>	<i>k</i> <sub>app</sub> × 10 <sup>3</sup>
1a	–	–	–	–	–	–	71.3	11 (98.9)
1b	–	–	–	–	–	+	183.2	
2a	+	–	–	–	–	–	173.9	5.4 (98)
2b	+	–	–	–	–	+	564	
3a	–	+	–	–	–	–	116.9	21.8 (98.6)
3b	–	+	–	–	–	+	229.9	
4a	+	+	–	–	–	–	476.5	16.5 (98.9)
4b	+	+	–	–	–	+	1066.8	
5a	–	–	+	–	–	–	85.7	12.6 (98.3)
5b	–	–	+	–	–	+	203.4	
6a	+	–	+	–	–	–	174.1	6 (98.5)
6b	+	–	+	–	–	+	570	
7a	–	+	+	–	–	–	135.4	25.3 (98.4)
7b	–	+	+	–	–	+	239	
8a	+	+	+	–	–	–	521.6	19.1 (98.7)
8b	+	+	+	–	–	+	1108.8	
9a	–	–	–	+	–	–	108.6	18.2 (98.8)
9b	–	–	–	+	–	+	224.5	
10a	+	–	–	+	–	–	236.8	7.1 (98.7)
10b	+	–	–	+	–	+	710.5	
11a	–	+	–	+	–	–	145.3	30.3 (98.8)
11b	–	+	–	+	–	+	242.8	
12a	+	+	–	+	–	–	604.9	21.5 (97.5)
12b	+	+	–	+	–	+	1160.8	
13a	–	–	+	+	–	–	116.9	19.8 (98.8)
13b	–	–	+	+	–	+	229.9	
14a	+	–	+	+	–	–	295.8	9.4 (98.9)
14b	+	–	+	+	–	+	825.5	
15a	–	+	+	+	–	–	159.8	35.6 (98.4)
15b	–	+	+	+	–	+	245.8	
16a	+	+	+	+	–	–	687	26.8 (99.2)
16b	+	+	+	+	–	+	1194.9	
17a	–	–	–	–	+	–	70.3	11.9 (97.9)
17b	–	–	–	–	+	+	183.2	
18a	+	–	–	–	+	–	174.1	5.2 (98.2)
18b	+	–	–	–	+	+	564	
19a	–	+	–	–	+	–	80.7	12.3 (98.3)
19b	–	+	–	–	+	+	197.5	
20a	+	+	–	–	+	–	295.8	8.8 (98.7)
20b	+	+	–	–	+	+	825.5	
21a	–	–	+	–	+	–	85.7	13.6 (98.5)
21b	–	–	+	–	+	+	194.2	
22a	+	–	+	–	+	–	174.1	6 (97.8)
22b	+	–	+	–	+	+	641.6	
23a	–	+	+	–	+	–	99.9	15.4 (98.6)
23b	–	+	+	–	+	+	217.6	
24a	+	+	+	–	+	–	426.4	13.1 (99)
24b	+	+	+	–	+	+	1017	
25a	–	–	–	+	+	–	108.6	20.4 (98.4)
25b	–	–	–	+	+	+	224.4	
26a	+	–	–	+	+	–	351.4	10.6 (96.9)
26b	+	–	–	+	+	+	916.1	
27a	–	+	–	+	+	–	80.7	25.3 (99.5)
27b	–	+	–	+	+	+	297.6	
28a	+	+	–	+	+	–	543.1	18.5 (98.2)
28b	+	+	–	+	+	+	1170.9	
29a	–	–	+	+	+	–	112.8	20.6 (98.7)
29b	–	–	+	+	+	+	227.3	
30a	+	–	+	+	+	–	428.7	14.8 (98.9)
30b	+	–	+	+	+	+	1017.8	
31a	–	+	+	+	+	–	142.1	30.5 (98.8)
31b	–	+	+	+	+	+	241.7	
32a	+	+	+	+	+	–	624.1	21.3 (98.6)
32b	+	+	+	+	+	+	1173.5	

influence degradation to a reasonable degree, while other interactions lie closer to the normal probability line and their effect may not be highly significant. This can evidently be illustrated in Fig. 3b where the effect of all parameters and their interactions is shown in the form of the Pareto chart; the ordinate shows the absolute

**Table 3**  
Estimated effects of the 2<sup>6</sup> factorial design for the removal of EP.

Effect	Value
Average effect	406.5 ± 1.85
<i>Main effects</i>	
EP concentration	481.7 ± 3.7
US density	172.6 ± 3.7
SPS	38.1 ± 3.7
pH <sub>0</sub>	115.1 ± 3.7
Matrix	-6.3 ± 3.7
Time	318.8 ± 3.7
<i>Two-factor interactions</i>	
(EP concentration) × (US density)	144.9 ± 3.7
(EP concentration) × (SPS)	27.3 ± 3.7
(EP concentration) × X(pH <sub>0</sub> )	82.9 ± 3.7
(EP concentration) × (Matrix)	4.6 ± 3.7
(EP concentration) × (Time)	202.4 ± 3.7
(US density) × (SPS)	5.6 ± 3.7
(US density) × (pH <sub>0</sub> )	-11.4 ± 3.7
(US density) × (Matrix)	-50.1 ± 3.7
(US density) × (Time)	24.3 ± 3.7
(SPS) × (pH <sub>0</sub> )	-0.8 ± 3.7
(SPS) × (Matrix)	8.2 ± 3.7
(SPS) × (Time)	-1.4 ± 3.7
(pH <sub>0</sub> ) × (Matrix)	35.8 ± 3.7
(pH <sub>0</sub> ) × (Time)	16.1 ± 3.7
(Matrix) × (Time)	13.2 ± 3.7
<i>Three-factor interactions</i>	
(EP concentration) × (US density) × (SPS)	5.1 ± 3.7
(EP concentration) × (US density) × (pH <sub>0</sub> )	-9 ± 3.7
(EP concentration) × (US density) × (Matrix)	-41.3 ± 3.7
(EP concentration) × (US density) × (Time)	21.8 ± 3.7
(EP concentration) × (SPS) × (pH <sub>0</sub> )	4.5 ± 3.7
(EP concentration) × (SPS) × (Time)	7.4 ± 3.7
(EP concentration) × (pH <sub>0</sub> ) × (Matrix)	29.7 ± 3.7
(EP concentration) × (Matrix) × (Time)	4.2 ± 3.7
(US density) × (SPS) × (pH <sub>0</sub> )	-15.1 ± 3.7
(US density) × (SPS) × (Matrix)	4.4 ± 3.7
(US density) × (SPS) × (Time)	-11.5 ± 3.7
(US density) × (pH <sub>0</sub> ) × (Matrix)	-0.3 ± 3.7
(US density) × (pH <sub>0</sub> ) × (Time)	-16.6 ± 3.7
(US density) × (Matrix) × (Time)	-0.3 ± 3.7
(SPS) × (pH <sub>0</sub> ) × (Matrix)	-11.1 ± 3.7
(SPS) × (pH <sub>0</sub> ) × (Time)	-9.8 ± 3.7
(SPS) × (Matrix) × (Time)	-1 ± 3.7
(pH <sub>0</sub> ) × (Matrix) × (Time)	11.7 ± 3.7

value of the effect, while the abscissa shows the main effects and the interactions. The vertical line shown in Fig. 3b is a reference line indicating the Lenth's pseudo-standard error; any effect that extends past this line is potentially significant [28].

Based on the parameters and interactions which are statistically significant (i.e. represented by white and black bars in Fig. 3b), a full model describing the experimental response was constructed as follows:

$$\begin{aligned}
 Y = & 406.5 + 240.9 \text{ EP concentration} + 86.3 \text{ US density} \\
 & + 19.1 \text{ SPS} + 57.6 \text{ pH}_0 + 159.4 \text{ Time} \\
 & + 72.5 \text{ EP concentration} * \text{US density} \\
 & + 13.7 \text{ EP concentration} * \text{SPS} + 41.5 \text{ EP concentration} \\
 & * \text{pH}_0 + 101.2 \text{ EP concentration} * \text{Time} \\
 & - 25.1 \text{ US density} * \text{Matrix} + 12.2 \text{ US density} * \text{Time} \\
 & + 17.9 \text{ pH}_0 * \text{Matrix} + 8.1 \text{ pH}_0 * \text{Time} \\
 & - 20.7 \text{ EP concentration} * \text{US density} * \text{Matrix} \\
 & + 10.9 \text{ EP concentration} * \text{US density} * \text{Time} \\
 & + 14.9 \text{ EP concentration} * \text{pH}_0 * \text{Matrix} \\
 & - 8.3 \text{ US density} * \text{pH}_0 * \text{Time}
 \end{aligned} \quad (\text{E2})$$

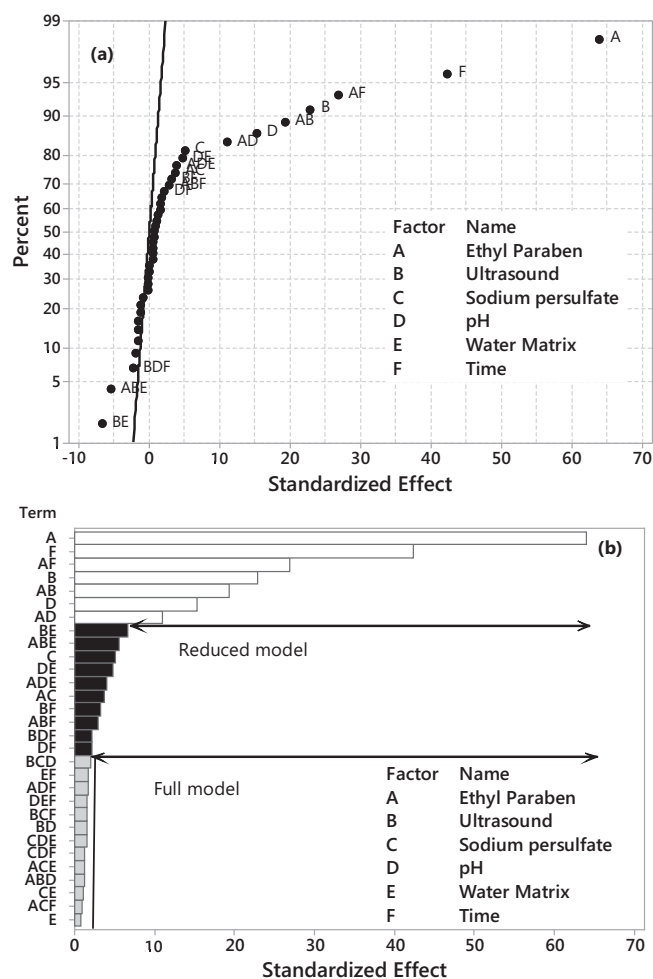


**Fig. 3.** Normal probability plot (a) and Pareto chart (b) of the effects for EP removal. White bars: effects of high significance; Black bars: effects of low significance; Gray bars: Non-significant effects.

The coefficients that appear in Eq. (E2) are half the calculated effects of Table 3, since a change from the low value (-1) to the upper value (+1) is a change of two units along the axis. The model predicts a linear dependency of the mass of EP removed on the operating parameters and the respective interactions. Usually, the three and higher order interactions are not expected to be significant. Their existence in the model indicates that the response surface is actually non-linear.

One of the objectives of the experimental design is to provide a simple and reliable model capable of relating directly the response factor to the most significant parameters. As seen in Fig. 3b, of the various effects that are statistically significant and appear in Eq. (E2), those shown as black bars are definitely less important than the rest (shown as white bars). To assess whether the model represented by Eq. (E2) may be simplified omitting these ten terms, the values of the residuals (i.e. observed minus predicted values of response) were plotted in a normal probability plot for both the full and the reduced models (Fig. 4). As seen, most of the points from the residual plot for the reduced model lie close to the straight line (confidence interval = 95%) confirming the conjecture that effects associated with the least significant terms of Eq. (E2) may be explained by random noise. The regression coefficient ( $R^2$ ) is 98.4% and 97.2% for the full and reduced model, respectively. Therefore, the experimental response of EP removal can be reduced and described as follows:

$$\begin{aligned}
 Y = & 406.5 + 240.9 \text{ EP concentration} + 86.3 \text{ US density} \\
 & + 19.1 \text{ SPS} + 57.6 \text{ pH}_0 + 159.4 \text{ Time} \\
 & + 72.5 \text{ EP concentration} * \text{US density} \\
 & + 13.7 \text{ EP concentration} * \text{SPS} + 41.5 \text{ EP concentration} \\
 & * \text{pH}_0 + 101.2 \text{ EP concentration} * \text{Time} \quad (\text{E3})
 \end{aligned}$$

The reduced model consists of seven positive effects, of which EP concentration is the most important one followed by the reaction time and their interaction, (EP concentration)  $\times$  (time). The beneficial effect of increasing power density has to do with an increase in the number of collapsing bubbles, thus leading to enhanced degradation levels [23]. The relatively low but still statistically significant effect of SPS (which appears in the full but not in the reduced model) may be associated with the fact that ultrasound can only partially activate SPS, as will be seen in Section 3.4. Interestingly and rather unexpectedly, the individual (main) effect of water matrix is insignificant at the conditions in question although higher order interactions such as (US density)  $\times$  (matrix), (pH<sub>0</sub>)  $\times$  (matrix), (US density)  $\times$  (matrix)  $\times$  (EP concentration) and (pH<sub>0</sub>)  $\times$  (matrix)  $\times$  (EP concentration) appear in the full model. The effluent organic matter, as well as the various anions typically found in WW are known to influence drastically the degradation kinetics of micro-pollutants. The impact is typically adverse [15,29,30] since the WW components behave as ROS scavengers competing with the substrate. Nonetheless, we have previously

reported [16] that estrogen sonodegradation in WW was faster than in UPW at pH 8 but the opposite occurred at pH 3, which shows that interactions might be significant. Sasi et al. [20] reported that methyl paraben sonochemical degradation was severely retarded in the presence of carbonates, while other anions such as chlorides, nitrates and sulfates had no effect. They also reported decreased degradation rates when methyl paraben was co-treated with other EDCs such as propyl paraben, phthalates and triclosan.

Regarding the effect of pH on EP sonochemical degradation, the rate was found to increase from acidic pH 3 to slightly alkaline pH 8. In general, the pH of the reaction medium has a complex effect on the sonochemical degradation rates of organic pollutants depending on the net charge (state) of the pollutant and the available amount of hydroxyl radicals and hydrogen peroxide (formed through radicals recombination) to attack the target pollutant [31,32]. Although at low pH values, EP molecules exist in non-ionic form (pK<sub>a</sub> = 8.22 [1]) and can easily approach the negatively charged cavity bubbles, better degradation efficiency of EP was observed in alkaline conditions. This can be attributed to the formation of stable H<sub>3</sub>O<sub>2</sub><sup>+</sup> cations resulting from the protonation of hydrogen peroxide, as well as to the scavenging of HO<sup>•</sup> radicals by H<sup>+</sup> at low pH values, limiting the degradation rate [31,32]. Thus, pH 8 could be considered as the reaction condition that counterbalances better both the formation of HO<sup>•</sup> radicals and the molecular form of EP, which can diffuse to the negatively charged hydrophobic interface of liquid–gas cavitation bubbles compared with pH 3.

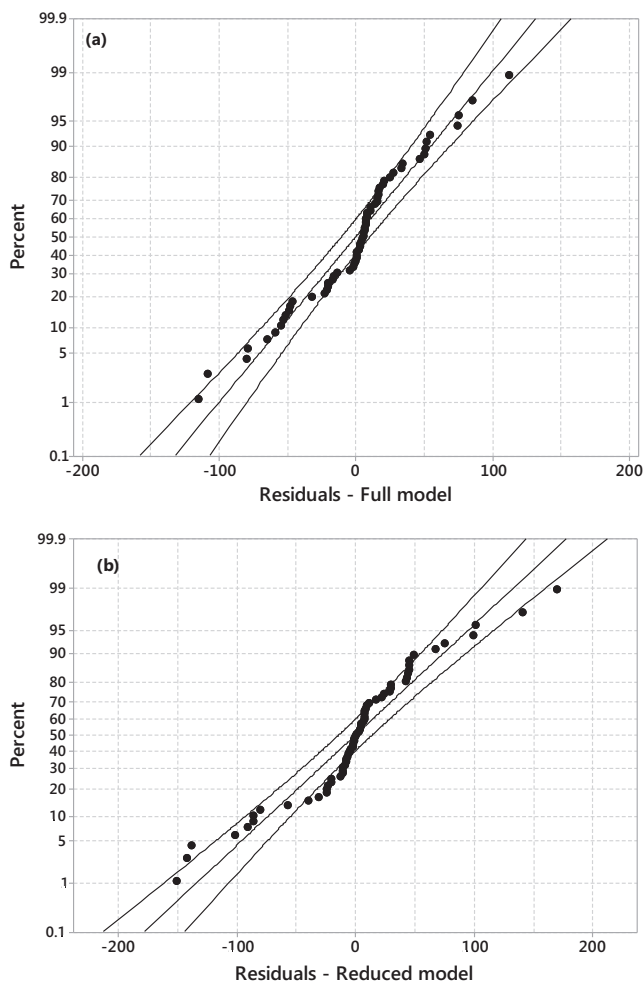


Fig. 4. Normal probability plots of the residuals for EP removal. Full model (a) and reduced model (b).

### 3.3. Kinetics

Although a detailed kinetic analysis was outside the scope of this work, an attempt was made to evaluate the reaction order with respect to EP. Besides the sampling times of 30 and 120 min used for factorial analysis, six extra samples were also taken at other intervals to obtain the EP concentration–time profiles for all the experiments (i.e. like those shown in Fig. 2). The respective data were then fitted to a pseudo-first order kinetic expression, as follows:

$$\begin{aligned}
 -dC/dt = k_{app}C & \Leftrightarrow \ln(C/C_0) = -k_{app}t \Leftrightarrow \ln(1 - X) \\
 & = -k_{app}t \quad (\text{E4})
 \end{aligned}$$

where  $k_{app}$  is an apparent rate constant and  $X$  is the conversion. The last column of Table 2 shows the computed rate constants, alongside the regression coefficients of linear fitting. Comparing experiments 1 and 2, 3 and 4, 5 and 6 and so on (i.e. experiments performed at low and high EP concentrations, while all other parameters are the same),  $k_{app}$  values change with EP concentration, which implies that the rate is not true first order regarding EP concentration. The fact that  $k_{app}$  consistently decreases with increasing concentration reveals that the reaction order is actually between one and zero. This can better be seen comparing conversion values. For the run 1 performed at 250  $\mu\text{g/L}$  EP, the 30-min and 120-min conversion is 28.5% and 73.3%, respectively, while for the run 2 performed at 1250  $\mu\text{g/L}$  EP, the respective values are 13.9% and 45.2%. If the reaction were true zero order, i.e.:

$$-dC/dt = k_{app} \Leftrightarrow C_0 - C = k_{app}t \Leftrightarrow X = k_{app}t/C_0 \quad (\text{E5})$$

a 5-fold increase in concentration would result in a 5-fold decrease in conversion. The fact that conversion and the rate constant decrease as concentration increases denotes kinetics between zeroth and first order.

At fixed operating conditions (i.e. ultrasound frequency and power density, liquid bulk temperature), the rate of ROS generation will be nearly constant and the kinetics of EP degradation will be

**Table 4**

High resolution accurate mass data ( $[M-H]^-$ , MS product ions and relative error  $\Delta$  (ppm) for EP and TBPs.

$R_t$ (min)	TBP	Pseudo-molecular formula	$m/z$ $[M-H]^-$	$\Delta$ (ppm)
7.9	Ethyl paraben (EP)	$C_9H_9O_3$	165.0551	3.4
6.9	Methyl paraben (MP)	$C_8H_7O_3$	151.0401	1.1
1.4	3,4 dihydroxybenzoic acid (3,4-DHB)	$C_7H_5O_4$	153.0200	4.5
1.6	2,4 dihydroxybenzoic acid (2,4-DHB)	$C_7H_5O_4$	153.0200	4.5
2.5	4 hydroxybenzoic acid (4-HB)	$C_7H_5O_3$	137.0244	-2.4

dictated by the ROS to EP concentration ratio. If this ratio is low (which may occur at high EP concentrations and/or conditions that do not favor the rapid ROS production), the reaction will approach zeroth order kinetics; conversely, a shift toward higher order kinetics is expected at higher ROS to EP ratios.

### 3.4. Identification of TBPs and degradation pathways

To identify TBPs, an additional 8-h long experiment was performed in the presence of 500 mg/L SPS and at an increased EP concentration of 3.5 mg/L to facilitate chromatographic analysis. The formation of TBPs was evaluated by means of LC-TOF-MS. Analyses were performed on pre-concentrated samples in full scan mode in order to facilitate the detection of as many TBPs as possible. Total ion chromatograms and filtered  $m/z$  chromatograms obtained after full-scan analyses of pre-concentrated samples indicated the formation of four TBPs (Table 4). Identification of TBPs (with the exception of methyl paraben) was also verified by comparison of retention times and MS spectra of the authentic reference standards in a second step.

One transformation product of EP with a molecular formula of  $C_8H_7O_3$  and pseudo-molecular  $[M-H]^-$  ion at  $m/z$  151.0401 was attributed to a dealkylated TBP and more specifically to methyl paraben (MP). Further dealkylation leads to the formation of one TBP eluting at 6.9 min with  $[M-H]^-$   $m/z$  137.0244 and elemental formula of  $C_7H_5O_3$ . Based on both literature data and comparison by authentic standards, TBP with  $m/z$  137.0244 is attributed to 4-hydroxybenzoic acid (4-HB).

Two more TBPs with isomeric structure were identified as dihydroxybenzoic acid (DHB) derivatives namely 2,4-DHB ( $m/z$  153.0200) and 3,4-DHB ( $m/z$  153.0200). Their identity was confirmed with the analysis of commercially available standards. Similar TBPs have been previously identified during the photocatalytic treatment of EP [12]. In agreement with our results, dealkylated and dihydroxybenzoic acids were the major TBPs during the treatment of compounds belonging also to the chemical category of para-hydroxybenzoates such as methyl and benzyl paraben by different advanced oxidation AOPs [33–35].

It is documented in the literature that  $HO^\cdot$  and  $SO_4^{\cdot-}$  can lead to the formation of similar TBPs though different mechanisms [15,36,37]. More specifically, hydroxylated-TBPs can be formed via the following mechanistic routes: (i) electrophilic attack of  $HO^\cdot$  radicals, and (ii) electron transfer from the aromatic ring to the  $SO_4^{\cdot-}$  generating radical cations. Subsequent reaction of radical cations with  $H_2O$  can generate hydroxycyclohexadienyl radicals through addition or elimination pathways. In both cases, the presence of electron-donating HO group in the substituted benzenes favors subsequent hydroxylation [15,36–39]. Similarly, dealkylated TBPs (i.e. MP) can be formed through the direct loss of  $-CH_3$  group of ethyl chain by  $HO^\cdot$  and  $SO_4^{\cdot-}$  attack. Alternatively, radical formation by hydrogen abstraction from the  $-CH_3$  group after  $HO^\cdot$  and

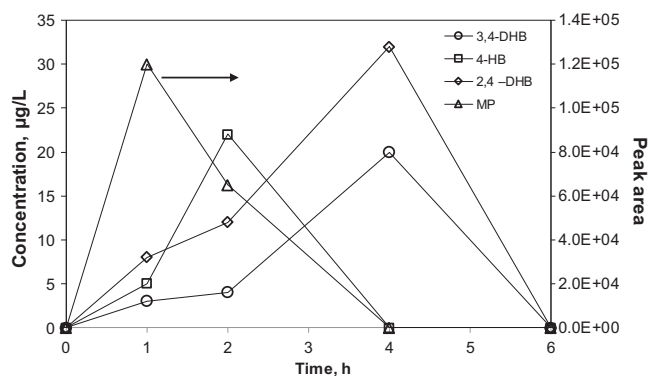


**Fig. 5.** Evolution profiles of TBPs during the sonochemical degradation of 3.5 mg/L EP in UPW, 20 W/L and 500 mg/L SPS. MP concentration is shown in secondary axis in terms of chromatographic peak area.

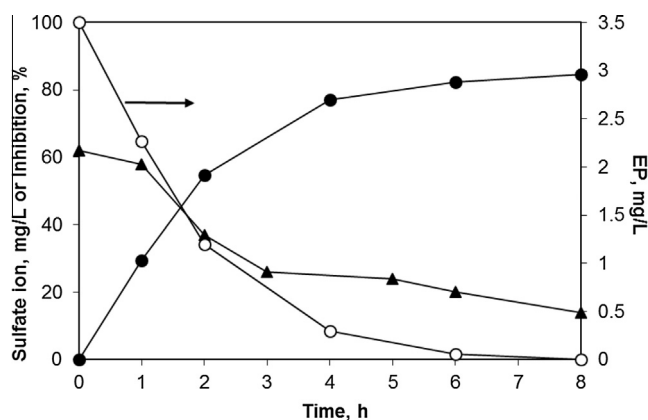


**Fig. 6.** Evolution of sulfate ion (●), EP (○) and toxicity (▲) at the conditions of Fig. 5.

$SO_4^{\cdot-}$  attack followed by addition of dissolved  $O_2$  and decarboxylation leads to dealkylated MP [15,35–40].

TBPs evolution as a function of treatment time was also followed. Fig. 5 shows the concentration–time profiles of 4-HB, 2,4-DHB and 3,4-DHB, whereas for MP the chromatographic peak area as a function of reaction time is depicted. All of them were readily transformed and completely removed after 6 h of ultrasound irradiation. Based on the profiles of Fig. 5, MP was found to be a first stage TBP of EP degradation attaining its maximum concentration within 1 h. 4-HB attained its maximum concentration within 2 h proving the consecutive steps of dealkylation. On the other hand, the formation of dihydroxybenzoic acids peak at longer irradiation times (4 h).

Fig. 6 shows the evolution of EP, sulfate ion and toxicity during the reaction; toxicity to *V. fischeri* decreases from 62% to 25% after 4 h of reaction and this coincides with 90% EP removal, thus implying that TBPs are less toxic than the parent compound. Interestingly, the measured concentration of sulfate ion at the end of the experiment corresponds to only 21% utilization of SPS and its sono-activated conversion to sulfate radicals.

Based on the detected TBPs and their evolution profiles, the sono-degradation pathway of EP is proposed in Fig. 7, including successive dealkylation of ethyl chain, followed by the hydroxylation of the aromatic ring leading to the formation of dihydroxybenzoic acids. This implies that hydroxyl radical-driven reactions play an important role in the process; these reactions are likely to occur in the neighborhood of the cavitation bubble and/or in the liquid

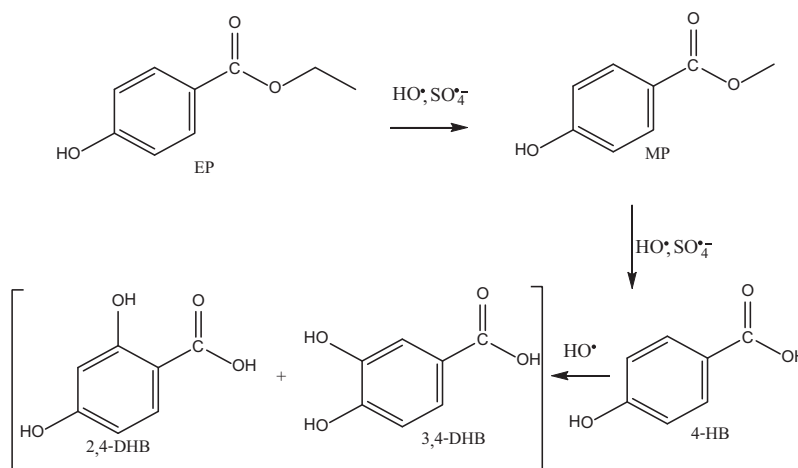


Fig. 7. Sonochemical degradation pathways of EP.

bubble, while thermal degradation inside the bubble is unlikely to happen given that EP is a water soluble and non-volatile species.

All the above intermediates can be further transformed by an oxidative opening of the aromatic ring via HO• and/or SO<sub>4</sub>•<sup>-</sup> continuous attack, giving rise to the formation of lower molecular weight and more oxidized molecules e.g. oxalic, formic, acetic, lactic, malonic, tartaric, glyceric and succinic acid, as reported elsewhere [36].

#### 4. Conclusions

Parabens constitute a new family of emerging micro-pollutants, whose advanced oxidation has merely been investigated so far. This is particularly true for their sonochemical degradation and, in this perspective, ethyl paraben was chosen as a representative compound to be studied. The main conclusions of this work are as follows:

- (1) To evaluate the importance of operating parameters on degradation, a factorial design approach was implemented. Six parameters, namely ethyl paraben concentration, reaction time, ultrasound power, initial pH, water matrix and the addition of sodium persulfate (as a source of sulfate radicals) were tested. Of primary importance were the first four, as well the second order interactions between concentration and each of the other three parameters. The effect of persulfate, although statistically significant, was less important than the others, while the water matrix effect was non-significant.
- (2) An empirical mathematical model capable of simulating quantitatively the amount of paraben removed was developed. The model contains the aforementioned four individual effects and the three second order interactions, while effects of lower significance were omitted to obtain a simplified (reduced) model without losing accuracy.
- (3) Such models should be viewed cautiously since they are applicable within the range of conditions they have been developed for. For this range, the rate of ethyl paraben sonochemical degradation obeys kinetics between 0th and 1st order with respect to concentration.
- (4) During the early steps of the reaction, ethyl paraben undergoes dealkylation to form methyl paraben, whose subsequent hydroxylation yields mono and dihydroxybenzoic acids.

#### Acknowledgement

This work was supported by Grant E056 from the Research Committee of the University of Patras (Program C. Caratheodory).

#### References

- [1] C. Haman, X. Dauchy, C. Rosin, J.F. Munoz, Occurrence, fate and behavior of parabens in aquatic environments: a review, *Water Res.* 68 (2015) 1–11.
- [2] E.J. Routledge, J. Parker, J. Odum, J. Ashby, J.P. Sumpter, Some alkyl hydroxy benzoate preservatives (parabens) are estrogenic, *Toxicol. Appl. Pharmacol.* 153 (1998) 12–19.
- [3] S. Oishi, Effects of butylparaben on the male reproductive system in rats, *Toxicol. Ind. Health* 217 (2001) 31–39.
- [4] P.D. Darbre, A. Aljarrah, W.R. Miller, N.G. Coldham, M.J. Sauer, G.S. Pope, Concentrations of parabens in human breast tumours, *J. Appl. Toxicol.* 24 (2004) 5–13.
- [5] D. Bledzka, J. Gromadzinska, W. Wasowicz, Parabens. From environmental studies to human health, *Environ. Int.* 67 (2014) 27–42.
- [6] I. Gonzalez-Marino, J.B. Quintana, I. Rodriguez, R. Cela, Evaluation of the occurrence and biodegradation of parabens and halogenated by-products in wastewater by accurate-mass liquid chromatography-quadrupole-time-of-flight-mass spectrometry (LC-QTOF-MS), *Water Res.* 45 (2011) 6770–6780.
- [7] J.R. Steter, R.S. Rocha, D. Dionisio, M.R.V. Lanza, A.J. Motheo, Electrochemical oxidation route of methyl paraben on a boron-doped diamond anode, *Electrochim. Acta* 117 (2014) 127–133.
- [8] L. Hernandez-Leal, H. Temmink, G. Zeeman, C.J.N. Buisman, Removal of micropollutants from aerobically treated grey water via ozone and activated carbon, *Water Res.* 45 (2011) 2887–2896.
- [9] D. Dobrin, M. Magureanu, C. Bradu, N.B. Mandache, P. Ionita, V.I. Parvulescu, Degradation of methylparaben in water by corona plasma coupled with ozonation, *Environ. Sci. Pollut. Res.* 21 (2014) 12190–12197.
- [10] D. Bledzka, D. Gryglik, M. Olak, J.L. Gebicki, J.S. Miller, Degradation of n-butylparaben and 4-tert-octylphenol in H<sub>2</sub>O<sub>2</sub>/UV system, *Radiat. Phys. Chem.* 79 (2010) 409–416.
- [11] P. Atheba, P. Drogui, B. Seyhi, D. Robert, Photo-degradation of butyl parahydroxybenzoate by using TiO<sub>2</sub>-supported catalyst, *Water Sci. Technol.* 67 (2013) 2141–2147.
- [12] A. Petala, Z. Frontistis, M. Antonopoulou, I. Konstantinou, D.I. Kondarides, D. Mantzavinos, Kinetics of ethyl paraben degradation by simulated solar radiation in the presence of N-doped TiO<sub>2</sub> catalysts, *Water Res.* 81 (2015) 157–166.
- [13] T. Velegraki, E. Hapeshi, D. Fatta-Kassinos, I. Poullos, Solar-induced heterogeneous photocatalytic degradation of methyl-paraben, *Appl. Catal. B Environ.* 178 (2015) 2–11.
- [14] R.A. Torres, C. Petrier, E. Combet, M. Carrier, C. Pulgarin, Ultrasonic cavitation applied to the treatment of bisphenol A. Effect of sonochemical parameters and analysis of BPA by-products, *Ultrason. Sonochem.* 15 (2008) 605–611.
- [15] B. Darsinou, Z. Frontistis, M. Antonopoulou, I. Konstantinou, D. Mantzavinos, Sono-activated persulfate oxidation of bisphenol A: Kinetics, pathways and the controversial role of temperature, *Chem. Eng. J.* 280 (2015) 623–633.
- [16] Z. Frontistis, D. Mantzavinos, Sonodegradation of 17 $\alpha$ -ethynylestradiol in environmentally relevant matrices: laboratory-scale kinetic studies, *Ultrason. Sonochem.* 19 (2012) 77–84.

- [17] G. Andaluri, E.V. Rokhina, R.P.S. Suri, Evaluation of relative importance of ultrasound reactor parameters for the removal of estrogen hormones in water, *Ultrason. Sonochem.* 19 (2012) 953–958.
- [18] M. Chiha, O. Hamdaoui, S. Baup, N. Gondrexon, Sonolytic degradation of endocrine disrupting chemical 4-cumylphenol in water, *Ultrason. Sonochem.* 18 (2011) 943–950.
- [19] L.J. Xu, W. Chu, N. Graham, A systematic study of the degradation of dimethyl phthalate using a high-frequency ultrasonic process, *Ultrason. Sonochem.* 20 (2013) 892–899.
- [20] S. Sasi, M.P. Rayaroth, D. Devadasan, U.K. Aravind, C.T. Aravindakumar, Influence of inorganic ions and selected emerging contaminants on the degradation of methylparaben: a sonochemical approach, *J. Hazard. Mater.* 300 (2015) 202–209.
- [21] R. Daghrir, A. Dimboukou-Mpira, B. Seyhi, P. Drogui, Photosonochemical degradation of butyl-paraben: optimization, toxicity and kinetic studies, *Sci. Total Environ.* 490 (2014) 223–234.
- [22] E.J. Routledge, J.P. Sumpter, Estrogenic activity of surfactants and some of their degradation products assessed using a recombinant yeast screen, *Environ. Toxicol. Chem.* 15 (1996) 241–248.
- [23] Y.G. Adewuyi, Sonochemistry: environmental science and engineering applications, *Ind. Eng. Chem. Res.* 40 (2001) 4681–4715.
- [24] S. Wang, N. Zhou, S. Wu, Q. Zhang, Z. Yang, Modeling the oxidation kinetics of sono-activated persulfate's process on the degradation of humic acid, *Ultrason. Sonochem.* 23 (2015) 128–134.
- [25] J.C. Lin, S.L. Lo, C.Y. Hu, Y.C. Lee, J. Kuo, Enhanced sonochemical degradation of perfluorooctanoic acid by sulfate ions, *Ultrason. Sonochem.* 22 (2015) 542–547.
- [26] G.E.P. Box, W.G. Hunter, J.S. Hunter, *Statistics for Experimenters*, John Wiley & Sons, New York, 1978.
- [27] C. Daniel, *Applications of Statistics to Industrial Experiments*, John Wiley & Sons, New York, 1976.
- [28] R.V. Lenth, Quick and easy analysis of unreplicated factorials, *Technometrics* 31 (1989) 469–473.
- [29] B. Li, L. Li, K. Lin, W. Zhang, S. Lu, Q. Luo, Removal of 1,1,1-trichloroethane from aqueous solution by a sono-activated persulfate process, *Ultrason. Sonochem.* 20 (2013) 855–863.
- [30] L. Sanchez-Prado, R. Barro, C. Garcia-Jares, M. Llompart, M. Lores, C. Petrakis, N. Kalogerakis, D. Mantzavinos, E. Psillakis, Sonochemical degradation of triclosan in water and wastewater, *Ultrason. Sonochem.* 15 (2008) 689–694.
- [31] M.V. Bagal, P.R. Gogate, Wastewater treatment using hybrid treatment schemes based on cavitation and Fenton chemistry: a review, *Ultrason. Sonochem.* 21 (2014) 1–14.
- [32] M. Lastre-Acosta, G. Cruz-González, L. Nuevas-Paz, U.J. Jáuregui-Haza, A.C. Silva Costa Teixeira, Ultrasonic degradation of sulfadiazine in aqueous solutions, *Environ. Sci. Pollut. Res.* 22 (2015) 918–925.
- [33] X. Feng, Y. Chen, Y. Fang, X. Wang, Z. Wang, T. Tao, Y. Zuo, Photodegradation of parabens by Fe(III)-citrate complexes at circumneutral pH: matrix effect and reaction mechanism, *Sci. Total Environ.* 472 (2014) 130–136.
- [34] Y. Gao, T. An, H. Fang, Y. Ji, G. Li, Computational consideration on advanced oxidation degradation of phenolic preservative, methylparaben, in water: mechanisms, kinetics, and toxicity assessments, *J. Hazard. Mater.* 278 (2014) 417–425.
- [35] Y. Lin, C. Ferronato, N. Deng, J.M. Chovelon, Study of benzylparaben photocatalytic degradation by TiO<sub>2</sub>, *Appl. Catal. B Environ.* 104 (2011) 353–360.
- [36] R. Hazime, Q.H. Nguyen, C. Ferronato, A. Salvador, F. Jaber, J.-M. Chovelon, Comparative study of imazalil degradation in three systems: UV/TiO<sub>2</sub>, UV/K<sub>2</sub>S<sub>2</sub>O<sub>8</sub> and UV/TiO<sub>2</sub>/K<sub>2</sub>S<sub>2</sub>O<sub>8</sub>, *Appl. Catal. B Environ.* 144 (2014) 286–291.
- [37] R. Hazime, Q.H. Nguyen, C. Ferronato, F. Jaber, J.-M. Chovelon, Optimization of imazalil removal in the system UV/TiO<sub>2</sub>/K<sub>2</sub>S<sub>2</sub>O<sub>8</sub> using a response surface methodology (RSM), *Appl. Catal. B Environ.* 132–133 (2013) 519–526.
- [38] M. Antonopoulou, I. Konstantinou, TiO<sub>2</sub> photocatalysis of 2-isopropyl-3-methoxy pyrazine taste and odor compounds in aquatic systems: kinetics, degradation pathways and toxicity evaluation, *Catal. Today* 240 (2015) 22–29.
- [39] M.G. Antoniou, A. De La Cruz, D.D. Dionysiou, Intermediates and reaction pathways from the degradation of microcystin-LR with sulfate radicals, *Environ. Sci. Technol.* 44 (2010) 7238–7244.
- [40] M.V.P. Sharma, V. Durgakumari, M. Subrahmanyam, Solar photocatalytic degradation of isoproturon over TiO<sub>2</sub>/H-MOR composite systems, *J. Hazard. Mater.* 160 (2008) 568–575.